Neutron-powder-diffraction study of the long-range order in the octahedral sublattice of $LaD_{2.25}$

T. J. Udovic
Materials Science and Engineering Laboratory, National Institute of Standards and Technology, Gaithersburg, Maryland 20899

Q. Huang
Materials Science and Engineering Laboratory, National Institute of Standards and Technology, Gaithersburg, Maryland 20899 and Department of Materials and Nuclear Engineering, University of Maryland, College Park, Maryland 20742

J. J. Rush
Materials Science and Engineering Laboratory, National Institute of Standards and Technology, Gaithersburg, Maryland 20899

J. Schefer
Laboratorium für Neutronenstreuung, Eidgenössische Technische Hochschule, Zürich & PSI Villigen, CH-5232 Villigen PSI, Switzerland

I. S. Anderson
Institut Laue-Langevin, 38042 Grenoble Cedex, France
(Received 19 August 1994; revised manuscript received 11 January 1995)

Neutron-powder-diffraction patterns of the superstoichiometric rare-earth dideuteride $LaD_{2.25}$ were measured between 15 and 400 K. Profile refinements indicated that, above ~345 K, the $LaD_{2.25}$ structure is cubic ($Fm3m$) with deuterium fully occupying the tetrahedral (t) interstices of the fcc La lattice and the excess deuterium occupying a portion of the octahedral (o) interstices with full statistical disorder. As the temperature is decreased below ~345 K, the $LaD_{2.25}$ structure undergoes a transformation to tetragonal symmetry concomitant with the onset of deuterium long-range order ($I4/mmm$) in the o sublattice. Fully developed long-range order is established near 230 K and ideally corresponds to the occupation of only those o sites within every fourth $(042)_{cubic}$ plane, in line with that reported for other rare-earth–deuterium systems possessing similar D/metal stoichiometric ratios. This ordering is accompanied by an outward expansion of the cubic ensemble of eight t-site deuterium atoms surrounding each o-site deuterium (D_o) atom. Moreover, the c-directed La-D_o bond distances are decreased by a displacement of the La atoms toward the D_o atoms.

INTRODUCTION

In the past, it was generally believed (e.g., Ref. 1) that the light rare-earth metal hydrides RH_{2+x} (where R = La, Ce, Pr, and Nd) possessed relatively simple phase diagrams. At $x=0$, the two tetrahedral (t) interstitial sites/metal atom present in the fcc metal lattice were occupied by hydrogen to form a CaF_2-like structure; for $x>0$, the additional hydrogen randomly occupied x octahedral (o) interstitial sites/metal atom up to a maximum concentration of $x=1$, at which point, every o site/metal atom was occupied to form a BiF_3-like structure. It later became apparent that this was an oversimplification, with a variety of studies (e.g., Refs. 2–15) indicating that the phase diagrams of these hydrides possessed an array of concentration- and temperature-dependent phase transitions involving tetragonal distortion and ordering within the octahedral sublattice (i.e., the interstitial lattice of octahedral sites).

There is some evidence that the octahedrally coordinated deuterium (D_o) atoms of both light- and heavy-rare-earth metal deuterides have similar ordering tendencies near $x=0.25$. For example, neutron-powder-diffraction (NPD) studies of both $CeD_{2.26}$ (Ref. 5) and the superstoichiometric heavy-rare-earth dideuteride β-TbD_{2+x} ($0.095 \le x \le 0.18$) (Ref. 16) have reported $I4/mmm$ symmetries, indicating identically ordered D_o-sublattice structures characterized by $[0,0,1]_C$ and $[1,0,\frac{1}{2}]_C$ wave vectors. (In this paper, cubic indices are designated by either the subscript C or no subscript; tetragonal indices are designated by the subscript T). The $I4/mmm$ structure has also been observed[17] for the rare-earth-like actinide NpD_{2+x} compounds ($x=0.13$ and 0.65). For TbD_{2+x},[16] the ordering was investigated as a function of concentration and temperature. At high temperature, the D_o sublattice possessed statistical disorder, although neutron vibrational spectroscopic measurements[18] suggested that short-range order could not be ruled out. At low temperature, perfect order in the D_o sublattice coincided with the superstoichiometric compound $TbD_{2.25}$, and was defined by full o-site occupation for every fourth (042) plane with all other (042) planes empty. It was pointed out[16] that the $I4/mmm$-ordered D_o atoms are completely surrounded by nearest-neighbor o-site vacancies, which is therefore reflective of the presence of a repulsive interaction between D_o atoms. The authors concluded that, although the phase diagrams of light- and heavy-rare-earth hydrides differed consider-

ably, the ordering tendencies seemed to be essentially similar.

These ordering tendencies were borne out by recent first-principles calculations[19,20] of hydrogen ordering in β-YH_{2+x}, yielding results (expected to be valid in other rare-earth systems) which indicated that the $I4/mmm$ (DO_{22}) structure is the stable configuration near $x=0.25$. This structure was found to be favored energetically over the $Pm\bar{3}m$ ($L1_2$) ordered structure. The geometry of these two structures differs mainly in that the third-nearest-neighbor H_o pairs (with separations of $\sqrt{3/2}a_C$) are present in the $I4/mmm$ structure, and the number of second-nearest-neighbor H_o pairs (with separations of a_C) is reduced. This suggested that the stability of the $I4/mmm$ structure is linked to the presence of relatively long-ranged interactions between H_o atoms, and that the effective third-nearest-neighbor H_o-H_o interaction could be attractive.

Heat capacity studies[7] of $La(D/H)_{2+x}$ ($-0.1 \leq x \leq 1.0$), have suggested that $La(D/H)_{2.25}$ is also a pure hydrogen-ordering phase. An NPD measurement[3] of the slightly more superstoichiometric $LaD_{2.30}$ (as well as $CeD_{2.29}$ and $PrD_{2.37}$) has indicated room-temperature D_o ordering with $I4_1md$ (as opposed to $I4/mmm$) symmetry, although it is not clear how much the sample homogeneity and stoichiometric accuracy were affected by metal impurities and synthesis methods used. Nevertheless, this type of ordering is generally associated with D/metal stoichiometric ratios near 2.50,[3,5] and at some point above a ratio of 2.25, one would indeed expect to see the development of $I4_1md$ symmetry. Different structural studies[9,13] of CeD_{2+x} ($0.18 \leq x \leq 0.29$) have even suggested that the ordering occurs via the lower-symmetry $I4$ space group. To help clarify whether or not $I4/mmm$ ordering in the octahedral sublattice is a general phenomenon for superstoichiometric rare-earth dihydrides having D(H)/metal ratios near 2.25, we undertook a detailed NPD study concerning the temperature-dependent structural behavior of carefully prepared $LaD_{2.25}$.

EXPERIMENTAL PROCEDURE

Synthesis of the $LaD_{2.25}$ sample followed a two-step procedure[18] similar to that established by Vajda, Daou, and Burger.[21] In the first step at 773 K, ~26.5 g of high-purity La (99.99 at.% metal purity, Johnson Matthey) were loaded with D_2 (Spectra Gases Research Grade) by gas-phase absorption in a quartz tube to a nominal D/La stoichiometry of 2.00, allowed to equilibrate for 16 h, and finally vacuum evacuated for 8 h to remove any excess octahedrally coordinated (o-site) deuterium, which is known to be unstable at this temperature,[21] thus forming the "ideal" $LaD_{2.00}$ stoichiometry. In this way, a pure-dideuteride "baseline" compound was established, to be used as the starting point for the continued synthesis of the superstoichiometric $LaD_{2.25}$ compound. This removed a large portion of the stoichiometric inaccuracy due to any contaminants in the starting material that might prevent associated La atoms from becoming deuterided. The nominal D(H)/metal stoichiometry of the baseline compound (i.e., after vacuum evacuation) was estimated to be ~1.99. In the second step, the pure dideuteride sample was loaded with additional D_2 at 773 K to form the superstoichiometric $LaD_{2.25}$ compound, allowed to cool slowly to 503 K over an 8 h period and equilibrated there for 10 h more, and finally vacuum evacuated concomitant with rapid cooling to room temperature. Next, the sample was transferred to a He-filled glove box, pulverized, and sealed in a cylindrical V tube (12 mm inner diam. × 50 mm ht.). During experiments, the sample was mounted in a temperature-controlled, closed-cycle He refrigerator.

The NPD measurements were performed at the Neutron Beam Split-Core Reactor at NIST using the high-resolution, 32-counter BT-1 diffractometer. The Cu(311) monochromator was used at a wavelength of 1.5391(1) Å. The horizontal divergences were 15, 20, and 7 min of arc for the in-pile, monochromatic-beam, and diffracted-beam collimators, respectively. Data were collected every 0.05° over a 2θ angular range of 5 to 165°. All profile refinements were carried out with the Rietveld method[22] using the GSAS program.[23] Neutron-scattering amplitudes used in the refinements were 8.27 fm for La and 6.67 fm for D.[23] Wavelength errors are not included in the standard deviations of the unit cells.

RESULTS AND DISCUSSION

Neutron-diffraction measurements were performed between 15 and 400 K. Temperature-dependent structural differences are clearly evident from a comparison of characteristic high- and low-temperature powder patterns in Fig. 1. In particular, the high-temperature patterns above 345 K could be completely indexed using a cubic cell with $a_C \approx 5.65$ Å. Based on the systematic absences of the (hkl) reflections where $h+k$, $h+l$, and $k+l \neq 2n$, the $Fm3m$ (No. 225) space group was assumed, in accordance with previous LaH_{2+x} structural studies.[13] The La atoms were located at $2a$ (0,0,0), D_t atoms at $8c$ ($\frac{1}{4},\frac{1}{4},\frac{1}{4}$), and D_o atoms disordered over the sites $2b$ ($\frac{1}{2}$,0,0). At 365 K, the refinement with this model gave good agreement parameters $R_p=6.60\%$, $R_{wp}=8.11\%$, and $\chi^2=1.45$. Below 345 K, some peaks showed splitting and additional weak superlattice peaks appeared. All lines readily indexed using an enlarged tetragonal unit cell with $a_T=a_C$ and $c_T \approx 2a_C$. The systematic absences of the $(hkl)_T$ reflections where $h+k+l \neq 2n$ indicated a body-center lattice. The presence of the reflections $(110)_T$ at $2\theta \sim 22.34°$ and $(114)_T$ at ~39.04° meant that the data were incompatible with the $I4_1md$ (No. 109) space group reported for $LaD_{2.30}$,[3] since the $(hhl)_T$ reflections where $2h+l \neq 4n$ are prohibited by $I4_1md$ space-group extinctions. Moreover, the structure could not be successfully refined with the lower-symmetry $I4$ space group as reported[9,13] for CeD_{2+x} ($0.18 \leq x \leq 0.29$).

In short, the data suggested that the low-temperature tetragonal $LaD_{2.25}$ phase possessed the symmetry of the $I4/mmm$ (No. 139) space group, in line with the $CeD_{2.26}$

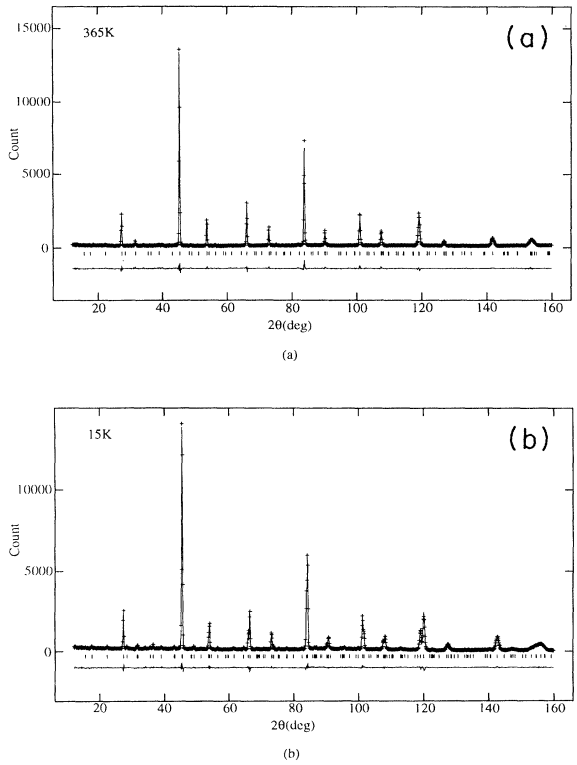

FIG. 1. (a) Cubic high-temperature (365 K, $Fm3m$) and (b) tetragonal low-temperature (15 K, $I4/mmm$) neutron-powder-diffraction patterns and corresponding fits (solid lines). The series of vertical lines below each pattern mark the calculated positions of Bragg reflections. The differences between calculated and observed intensities are also plotted below each pattern.

(Ref. 5) and TbD_{2+x} (Ref. 16) structural studies. In the first $I4/mmm$ refinement for the 15 K data, the La atoms, located at (0,0,0) in the cubic unit cell, were split into the positions La(1) at 4e (0,0,z) (with $z=\frac{1}{4}$) and La(2) at 4c ($\frac{1}{2}$,0,0); the D_o atoms, located at ($\frac{1}{2}$,0,0) in the cubic cell, were split into D(o1) at 2a (0,0,0), D(o2) at 2b ($\frac{1}{2}$,$\frac{1}{2}$,0), and D(o3) at 4d ($\frac{1}{2}$,0,$\frac{1}{4}$); and finally, the D_t atoms were located at the D(t) position 16n (x,x,z) with $x=\frac{1}{4}$ and $z=\frac{1}{8}$. The refinement with these special positions yielded agreement parameters $R_p=6.18\%$, $R_{wp}=8.19\%$, and $\chi^2=1.55$. A better model fit was obtained by allowing the atomic coordinates z for La(1) and x and z for D(t), and the occupancy parameters for D(o1), D(o2), D(o3), and D(t) to vary in the subsequent refinement. This yielded atomic coordinates $z=0.02459(2)$ for La(1), and $x=0.2593(2)$ and $z=0.1267(2)$ for D(t); and occupancy parameters $n_{D(o1)}\approx 1$, $n_{D(o2)}\approx 0.06$, $n_{D(o3)}\approx 0$, and $n_{D(t)}\approx 1$. The resulting agreement parameters were $R_p=5.97\%$, $R_{wp}=7.79\%$ and $\chi^2=1.40$. This refinement model also gave reasonable structural parameters except for the large temperature factors for the D_o atoms (2.1 Å^2 at 15 K and 3.2 Å^2 at 365 K). A second refinement model that used an anisotropic D_o temperature factor showed that the D_o atoms may be shifted from their ideal positions. This led to a third refinement model that used an isotropic D_o temperature factor yet allowed for a shift of the D_o atoms. The results of calculations with the isotropic (I), anisotropic (II), and shifted-atom (III) models are shown in Table I.

The refinement using model III with the 15 K data resulted in an off-center displacement of the D_o atoms that was 0.135 Å in the a and b directions and 0.090 Å in the c direction, and a much smaller temperature factor of 0.69 Å^2. All three models resulted in comparably good fits, and based on these results we could not determine unequivocally by NPD whether the D_o atoms were situated at the center of the o sites with large thermal motion (isotropic or anisotropic) or were actually situated randomly at one of the eight off-center locations associated with each o site with smaller thermal motion. One can expect a light atom such as D to undergo significant thermal motions when placed in the relatively large o sites of the $LaD_{2.25}$ lattice (e.g., compare it to the 0.98 Å^2 temperature factor found for D_t atoms in the smaller t sites). If on the other hand, the D_o atoms were shifted off-center, no correlations between D_o atoms in particular off-center locations were evident from the profile refinements. This is somewhat contrary to earlier NPD studies of $LaD_{2.30}$ (Ref. 3) and $LaH_{2.1}$,[24] where refinements of the models suggested that the H_o and D_o atoms were displaced along the [111] directions. Yet, this behavior may very well be the case for samples with D(H)/metal stoichiometric ratios deviating from 2.25, since these deviations will result in extra o-site vacancies or occupations, which in turn will locally perturb the axial symmetry of the o sites (see Fig. 3) afforded by the perfectly ordered $LaD_{2.25}$ structure. Hence, for reasons of simplicity and the presence of the axially symmetric tetragonal local environment surrounding the o sites, which would argue against off-center D_o positions, we have decided to use model I in our analyses of the $LaD_{2.25}$ data.

The results of the model-I profile refinements for all the NPD data are given in Tables II–IV. Figure 1 shows the agreement between observed and calculated intensities for both cubic and tetragonal models. For the 340 K data, neither tetragonal superlattice peaks nor peak splitting were readily evident. As a result, both the cubic and tetragonal models were used in the refinements. As shown in Table II, the tetragonal model gave a significantly better result than the cubic model, and thus, the $I4/mmm$ symmetry was adopted for the 340 K structure.

It should be noted that throughout the profile refinements, the different deuterium occupancy parameters (n_D) were not constrained to match the overall stated D/La stoichiometric ratio. The initial refinements indicated that at the lower temperatures, D(o3) and D(t) sites were found to be essentially vacant and fully occupied, respectively. Therefore, $n_{D(o3)}$ was fixed at 0 below 230 K, and $n_{D(t)}$ was fixed at 1 below 340 K. Otherwise, the deuterium occupancy parameters were allowed to vary, thus providing a refinement-generated check of the supposed sample stoichiometry.

TABLE I. The refinement results for different structural models of $LaD_{2.25}$ at 15 and 365 K.

		15 K			365 K		
		I	II	III	I	II	III
	S.G.	*I4/mmm*	*I4/mmm*	*I4/mmm*	*Fm3m*	*Fm3m*	*Fm3m*
	a (Å)	5.6174(1)	5.6175(1)	5.6175(1)	5.6442(1)	5.6442(1)	5.6442(1)
	c (Å)	11.3054(3)	11.3055(3)	11.3056(3)			
La(1)	x	0	0	0	0	0	0
	y	0	0	0	0	0	0
	z	0.2459(2)	0.2461(2)	0.2461(2)	0	0	0
	B (Å^2)	0.05(1)	0.05(2)	0.05(2)	0.62(3)	0.65(3)	0.66(3)
	n	1	1	1	1	1	1
La(2)	x	1/2	1/2	1/2			
	y	0	0	0			
	z	0	0	0			
	B (Å^2)	0.05(1)	0.05(2)	0.05(2)			
	n	1	1	1			
D($o1$)	x	0	0	0.024(1)	1/2	1/2	0.526(1)
	y	0	0	0.024(1)	0	0	0.026(1)
	z	0	0	0.008(1)	0	0	0.026(1)
	B (Å^2)[a]	2.1(1)		0.69	3.3(2)		1.20
	B_{11} (Å^2)[a]		2.4(2)			3.2(2)	
	B_{22} (Å^2)[a]		$=B_{11}$			$=B_{11}$	
	B_{33} (Å^2)[a]		1.4(2)			$=B_{11}$	
	n	0.98(2)	0.97(2)	0.121	0.269(7)	0.268(7)	
D($o2$)	x	1/2	1/2	0.524(1)			
	y	1/2	1/2	0.524(1)			
	z	0	0	0.008(1)			
	n	0.06(1)	0.05(1)	0.007(1)			
D(t)	x	0.2593(2)	0.2592(2)	0.2592(2)	1/4	1/4	1/4
	y	0.2593(2)	0.2592(2)	0.2592(2)	1/4	1/4	1/4
	z	0.1267(2)	0.1267(2)	0.1267(2)	1/4	1/4	1/4
	B (Å^2)	0.98(3)	0.99(3)	0.98(3)	1.62(4)	1.62(4)	1.60(4)
	n	1	1	1	0.991(7)	0.989(8)	0.986(8)
	R_p (%)	5.97	5.91	5.90	6.60	6.61	6.55
	R_{wp} (%)	7.79	7.72	7.71	8.11	8.15	8.07
	χ^2	1.40	1.38	1.37	1.45	1.46	1.44

[a]Constrain: B [La(1)]$=B$ [La(2)],B [D($o1$)]$=B$ [D($o2$)], B_{11}[D($o1$)]$=B_{22}$ [D($o1$)]$=B_{11}$[D($o2$)] $=B_{22}$[D($o2$)], and B_{33}[D($o1$)]$=B_{33}$[D($o2$)]. Note: at 15 K, D($o3$) sites were found to be unoccupied.

TABLE II. Lattice parameters for $LaD_{2.25}$.

T (K)	Space group	a (Å)	c (Å)	V (Å^3)	c/a	R_p (%)	R_{wp} (%)	χ^2
15	*I4/mmm*	5.6174(1)	11.3054(3)	356.74(2)	2.0126	5.97	7.79	1.40
80		5.6180(1)	11.3060(3)	356.84(2)	2.0125	5.73	7.16	1.23
150		5.6215(1)	11.3094(3)	357.39(2)	2.0118	5.58	7.17	1.39
200		5.6240(1)	11.3110(3)	357.77(2)	2.0112	5.44	7.04	1.34
225		5.6261(1)	11.3114(3)	358.04(2)	2.0105	5.42	7.06	1.35
230		5.6262(1)	11.3115(3)	358.05(2)	2.0105	5.38	7.04	1.34
240		5.6262(1)	11.3098(3)	358.00(2)	2.0102	4.94	6.29	1.15
250		5.6284(1)	11.3094(3)	358.27(2)	2.0093	5.60	7.18	1.39
260		5.6276(1)	11.3076(3)	358.11(2)	2.0093	4.98	6.39	1.11
275		5.6311(1)	11.3065(3)	358.52(2)	2.0079	5.42	6.96	1.31
290		5.6337(1)	11.3043(3)	358.78(2)	2.0066	5.96	7.52	1.52
300		5.6352(1)	11.3017(3)	358.89(2)	2.0056	5.58	7.18	1.38
315		5.6384(2)	11.2980(5)	359.18(3)	2.0038	6.87	9.66	1.99
340		5.6400(2)	11.2931(5)	359.23(3)	2.0023	4.67	6.09	2.20
	Fm3m	5.6438(1)		179.77(1)		6.50	8.24	3.59
350		5.6438(1)		179.77(1)		5.93	7.13	1.58
365		5.6442(1)		179.80(1)		6.60	8.11	1.45
380		5.6469(1)		180.06(1)		5.89	7.42	1.36
400		5.6512(1)		180.476(9)		5.50	6.99	1.20

TABLE III. Atomic parameters for $LaD_{2.25}$. (Top) 15 K $\leq T \leq$ 340 K, space group: $I4/mmm$ (No. 139), atomic positions: La(1): $4e(0,0,z)$, La(2): $4c(1/2,0,0)$, D($o1$): $2a(0,0,0)$, D($o2$): $2b(1/2,1/2,0)$, D($o3$): $4d(1/2,0,1/4)$, D(t): $16n(x,x,z)$. The occupancy parameters are fixed at 1 for La(1) and La(2), 1 for D(t) below 340 K, and 0 for D($o3$) below 230 K. (Bottom) 350 K $\leq T \leq$ 400 K, space group: $Fm3m$ (No. 225), atomic positions: La: $4a(0,0,0)$, D(o): $4b(1/2,0,0)$, and D(t): $8c(1/4,1/4,1/4)$.

T (K)	La(1)		La(2)	D($o1$)		D($o2$)		D($o3$)		D(t)				D/La
	z	B (Å^2)	B (Å^2)[a]	B (Å^2)[b]	n	B (Å^2)	n	B (Å^2)	n	x	z	B (Å^2)	n	
15	0.2459(2)	0.05(1)	0.05(1)	2.1(1)	0.98(2)	2.1(1)	0.06(1)			0.2593(2)	0.1267(2)	0.98(3)	1	2.260(7)
80	0.2463(2)	0.08(2)	0.08(2)	2.0(1)	0.99(1)	2.0(1)	0.05(1)			0.2591(2)	0.1269(2)	1.02(3)	1	2.260(5)
150	0.2458(2)	0.19(2)	0.19(2)	2.3(1)	1.00(1)	2.3(1)	0.06(1)			0.2592(2)	0.1262(2)	1.09(3)	1	2.265(5)
200	0.2460(2)	0.27(2)	0.27(2)	2.4(1)	1.00(1)	2.4(1)	0.07(1)			0.2588(2)	0.1263(2)	1.20(3)	1	2.268(5)
225	0.2462(2)	0.32(2)	0.32(2)	2.6(1)	0.99(2)	2.6(1)	0.09(1)			0.2594(2)	0.1261(2)	1.20(2)	1	2.270(7)
230	0.2462(2)	0.32(2)	0.32(2)	2.6(1)	0.99(2)	2.6(1)	0.09(1)	2.6(1)	0.00(1)	0.2594(2)	0.1261(2)	1.20(2)	1	2.270(7)
240	0.2463(2)	0.37(2)	0.37(2)	2.4(1)	0.96(2)	2.4(1)	0.07(1)	2.4(1)	0.01(1)	0.2588(2)	0.1269(2)	1.27(3)	1	2.26(1)
250	0.2463(2)	0.38(2)	0.38(2)	2.5(1)	0.94(2)	2.5(1)	0.09(1)	2.5(1)	0.01(1)	0.2589(2)	0.1261(2)	1.32(3)	1	2.26(1)
260	0.2466(2)	0.43(2)	0.43(2)	2.7(1)	0.98(2)	2.7(1)	0.07(1)	2.7(1)	0.01(1)	0.2590(2)	0.1264(2)	1.25(2)	1	2.27(1)
275	0.2465(2)	0.42(2)	0.45(2)	2.8(2)	0.91(2)	2.8(2)	0.09(1)	2.8(2)	0.03(1)	0.2589(2)	0.1260(2)	1.34(3)	1	2.27(1)
290	0.2467(2)	0.45(2)	0.45(2)	2.8(2)	0.89(2)	2.8(2)	0.11(2)	2.8(2)	0.03(1)	0.2585(2)	0.1257(3)	1.35(3)	1	2.27(2)
300	0 2447(3)	0.47(2)	0.47(2)	2.8(2)	0.85(2)	2.8(2)	0.11(2)	2.8(2)	0.05(1)	0.2583(2)	0.1253(3)	1.42(4)	1	2.27(2)
315	0.2480(5)	0.58(3)	0.58(3)	3.3(2)	0.78(2)	3.3(2)	0.16(2)	3.3(2)	0.08(1)	0.2562(4)	0.1252(5)	1.43(4)	1	2.28(2)
340	0.2488(7)	0.55(2)	0.55(2)	3.0(2)	0.50(3)	3.0(2)	0.30(3)	3.0(2)	0.13(1)	0.2534(5)	0.1250(4)	1.54(3)	1.00(1)	2.27(2)

T (K)	La		D(o)		D(t)		D/La
	B (Å^2)	n	B (Å^2)	n	B (Å^2)	n	
350	0.62(3)	1	3.3(2)	0.268(7)	1.64(5)	0.991(8)	2.25(2)
365	0.65(3)	1	3.2(2)	0.269(7)	1.62(4)	0.991(7)	2.25(2)
380	0.64(2)	1	3.7(2)	0.276(6)	1.59(4)	0.988(7)	2.25(2)
400	0.73(2)	1	4.1(2)	0.280(6)	1.76(4)	0.989(7)	2.26(2)

[a]Constrained temperature factors: B[La(2)] = B[La(1)].
[b]Constrained temperature factors: B[D($o1$)] = B[D($o2$)] = B[D($o3$)].

TABLE IV. Selected interatomic distances (Å) and angles (°). (Top) D_o-La distances. (Bottom) D_t-La distances (Å) and La-D_t-La angles (°).

T (K)	D($o1$)-La(1) (×2)	D($o1$)-La(2) (×4)	D($o2$)-La(1) (×2)	D($o2$)-La(2) (×4)	D($o3$)-La(1) (×2)	D($o3$)-La(2) (×4)
15	2.780(2)	2.80869(6)	2.872(2)	2.80869(6)		
80	2.785(2)	2.80900(6)	2.869(2)	2.80900(6)		
150	2.780(2)	2.81074(6)	2.875(2)	2.81074(6)		
200	2.782(2)	2.81202(6)	2.874(2)	2.81202(6)		
225	2.785(2)	2.81305(6)	2.871(2)	2.81305(6)		
230	2.785(2)	2.81309(6)	2.871(2)	2.81309(6)	2.81342(7)	2.82788(6)
240	2.785(2)	2.81308(5)	2.870(2)	2.81308(5)	2.81340(6)	2.82746(6)
250	2.785(3)	2.81421(6)	2.869(3)	2.81421(6)	2.81452(7)	2.82734(7)
260	2.788(2)	2.81381(6)	2.866(2)	2.81381(6)	2.81408(7)	2.82690(6)
275	2.787(3)	2.81557(6)	2.966(3)	2.81557(6)	2.81585(7)	2.82661(7)
290	2.789(3)	2.81683(6)	2.863(3)	2.81683(6)	2.81707(8)	2.82608(8)
300	2.796(3)	2.81761(6)	2.855(3)	2.81761(6)	2.81776(7)	2.82542(8)
315	2.802(5)	2.81922(8)	2.847(5)	2.81922(8)	2.81930(9)	2.82145(1)
340	2.810(7)	2.8200(1)	2.837(7)	2.8200(1)	2.8201(1)	2.8233(1)

Cubic	D(o)-La
350	2.82191(6)
365	2.82208(7)
380	2.82342(5)
400	2.82559(5)

TABLE IV. (*Continued*).

T (K)	D(t)-La(1)	D(t)-La(1)	D(t)-La(2) (×2)	La(1)-D(t)-La(1)	La(1)-D(t)-La(2) (×2)	La(1)-D(t)-La(2) (×2)	La(2)-D(t)-La(2)
15	2.462(2)	2.394(2)	2.450(1)	109.82(7)	107.16(4)	112.07(4)	108.33(7)
80	2.462(2)	2.391(2)	2.451(1)	109.91(7)	107.23(4)	112.00(4)	108.24(7)
150	2.464(2)	2.399(2)	2.449(1)	109.68(8)	107.15(4)	112.06(4)	108.51(8)
200	2.464(2)	2.402(2)	2.449(1)	109.65(8)	107.25(4)	111.95(4)	108.58(8)
225	2.471(2)	2.398(2)	2.449(1)	109.62(8)	107.13(4)	112.05(4)	108.63(8)
230	2.471(2)	2.398(2)	2.449(1)	109.62(8)	107.13(4)	112.04(4)	108.62(8)
240	2.462(2)	2.397(2)	2.454(1)	109.96(8)	107.27(5)	111.90(4)	108.33(8)
250	2.469(2)	2.401(2)	2.449(1)	109.64(10)	107.24(5)	111.91(5)	108.68(9)
275	2.472(3)	2.401(3)	2.449(2)	109.64(10)	107.26(4)	111.87(4)	108.77(10)
290	2.473(3)	2.405(3)	2.448(2)	109.54(13)	107.36(5)	111.73(5)	108.94(12)
300	2.479(3)	2.404(3)	2.445(2)	109.41(13)	107.45(5)	111.61(5)	109.13(13)
315	2.470(5)	2.414(5)	2.445(3)	109.46(20)	107.96(8)	111.07(8)	109.23(20)
340	2.457(5)	2.429(5)	2.444(2)	109.42(15)	108.64(16)	110.36(16)	109.38(15)
Cubic	D(t)-La (×4)				La-D(t)-La (×6)		
350	2.44384(4)				109.471(1)		
365	2.44400(4)				109.471(1)		
380	2.44516(3)				109.471(1)		
400	2.44704(3)				109.471(1)		

The final refinements indicate that, at high temperatures above ~345 K, the $LaD_{2.25}$ structure is cubic ($Fm3m$), and the D_o sublattice exhibits full statistical disorder. As the temperature is lowered below ~345 K, the $LaD_{2.25}$ structure undergoes a tetragonal distortion concomitant with the appearance and growth of superlattice lines (see Fig. 2). This is indicative of the onset and development of long-range order ($I4/mmm$) in the D_o sublattice, with D atoms ideally occupying only the o sites associated with every fourth (042) [or $(044)_T$ tetragonal equivalent] plane, identical to that observed for $CeD_{2.26}$ (Ref. 5) and TbD_{2+x}.[16]

Schematics of the $LaD_{2.25}$ structure at high and low temperature are illustrated in Fig. 3. Figure 3(a) shows the unit cell representing the high-temperature fluorite structure with full cubic symmetry and randomly occupied o sites. Figure 3(b) shows the doubled unit cell of the low-temperature ordered structure. In the ideally ordered D_o sublattice, all D($o1$) sites are occupied, while all D($o2$) and D($o3$) sites are vacant. The La atoms in the La(1) sites are shifted in the c direction toward the occupied D($o1$) sites. Since these La atoms have only one adjacent D_o atom, they are expected to relax toward the D_o atom to lower the system energy.[20] The tetrahedrally coordinated deuterium (D_t) atoms are shifted away from the center of the t sites as shown in Figs. 3(b) and 3(c). The net effect is an expansion of the cubes of eight D_t atoms surrounding the occupied D($o1$) sites, suggesting a repulsive D_o-D_t interaction. These La(1) and D(t) site displacements are similar to those reported[5] for the related light-rare-earth deuteride $CeD_{2.26}$. Figure 3(d) illustrates the (042) planes that identify the o sublattice, each plane labeled by the type of o site that it contains. In this way, the o sublattice can be described as a repeating series of four (042) planes in the order -D($o1$)-D($o3$)-D($o2$)-D($o3$)-. In the ideally ordered state, only the

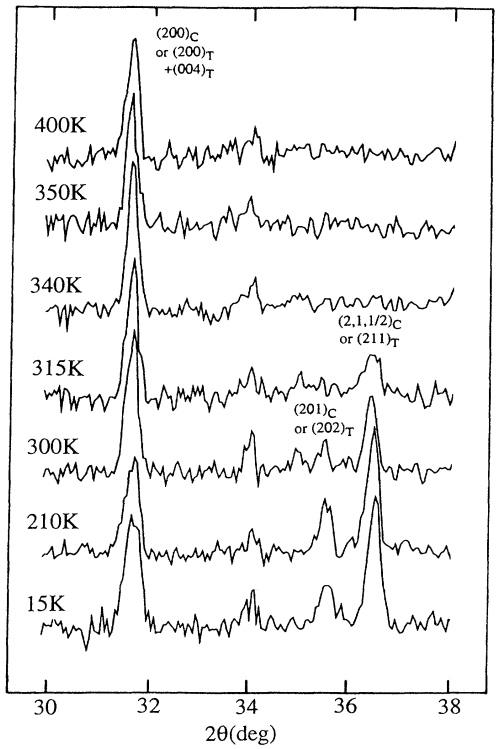

FIG. 2. The characteristic growth with decreasing temperature of the strongest superlattice reflection $(2,1,\frac{1}{2})_C$ $[(211)_T]$ compared to the $(200)_C$ and corresponding tetragonal $(200)_T$ and $(004)_T$ lattice reflections. Note that the relative intensity of the $(202)_T$ lattice reflection is also temperature dependent, being sensitive to the tetragonality, and decreases to zero intensity for the symmetry-forbidden $(201)_C$ equivalent reflection at high temperature. The temperature-independent weak feature at $2\theta \approx 34°$, with an intensity ~0.5% as large as that of the strongest lattice reflection $(220)_C$, is an impurity peak that could not be indexed.

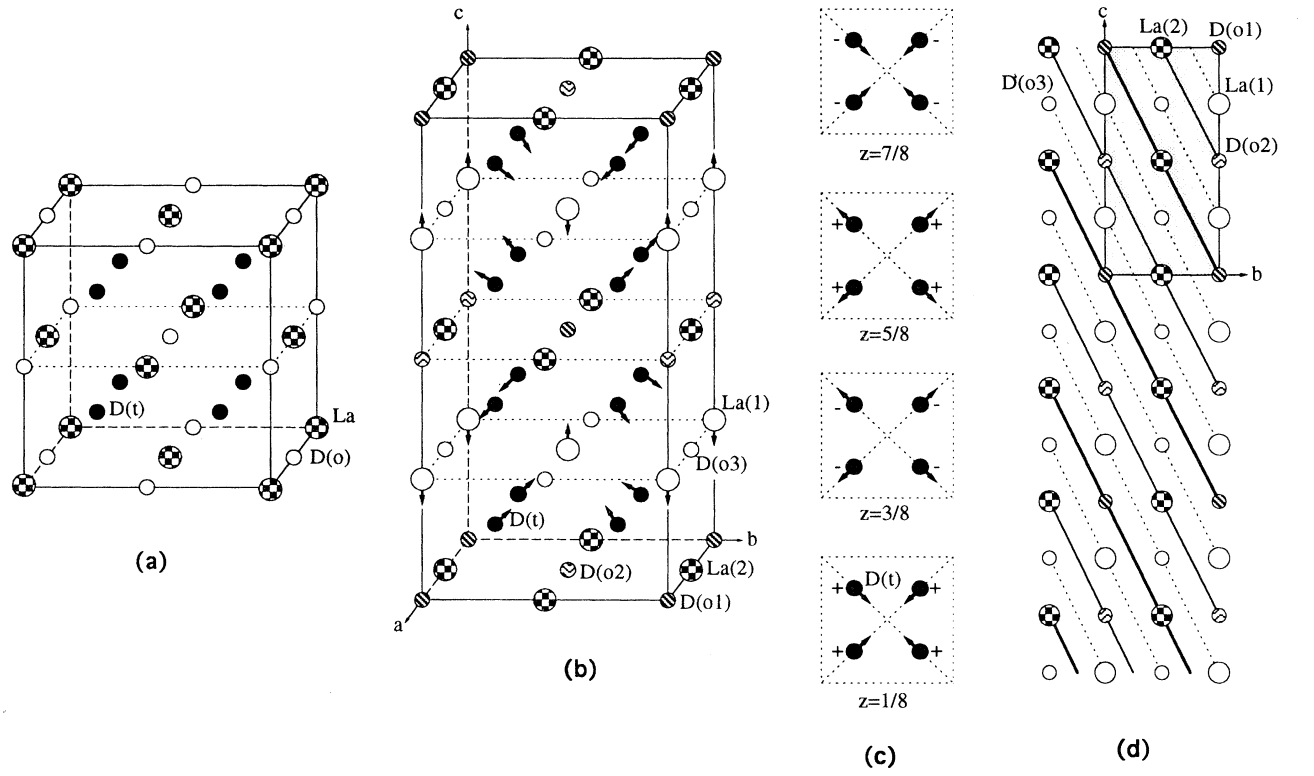

FIG. 3. Schematic of the $LaD_{2.25}$ structure at (a) high temperature ($Fm3m$) and (b) low temperature ($I4/mmm$); arrows indicate the displacement directions of the D_t and La atoms from the ideal $D(t)$ and La(1) positions, respectively. (c) basal-plane projections of the low-temperature D_t-atom displacements. (d) the series of (042) planes (labeled by the type of sites they contain) that comprise the o sublattice, with the a axis normal to the page. The t sites are excluded for clarity.

$D(o1)$ planes are occupied. With this arrangement, the twelve nearest-neighbor o sites (i.e., four $D(o2)$ and eight $D(o3)$ sites) surrounding each occupied $D(o1)$ site are vacant, an observation which prompted the authors of the TbD_{2+x} study[16] to suggest that a repulsive interaction between D_o atoms drives the D_o ordering.

As alluded to earlier, the low-temperature deuterium occupancy parameters in Tables I and III indicate slight deviations from ideal ordering. In particular, the fits show that, in addition to the full occupation of $D(o1)$ sites, 5–6% of the ideally vacant $D(o2)$ sites are randomly occupied at low temperature for this sample. This can be explained by the slightly high D/La ratios determined from the D occupancy parameters, which suggest that the true stoichiometry of the synthesized sample may be closer to $LaD_{2.26}$. (This possibility should be kept in mind throughout the paper although we will continue to refer to the sample as $LaD_{2.25}$.) The data suggest that the $D(o2)$ planes, which lie midway between the fully occupied $D(o1)$ planes and separated from them by empty $D(o3)$ planes [see Fig. 3(d)], are the preferred planes for additional D_o occupation once the D concentration is increased above the ideal D/La stoichiometry of 2.25. The deviation from ideal ordering was even more pronounced for $CeD_{2.26}$ (Ref. 5) where the authors suggested that the $D(o1)$, $D(o2)$, and $D(o3)$ planes were 97, 3, and 13% occupied, respectively, at 90 K. This apparent disorder is again probably due to the presence of significant sample impurities (since the starting metal purity was only 99.5%) leading to uncertain stoichiometry, higher intrinsic disorder, and possible inhomogeneity (where the value of x varies significantly throughout the sample). Moreover, the partial occupation of the $D(o3)$ planes is contrary to the vacant $D(o3)$ planes suggested by the refinements of the $LaD_{2.25}$ data, yet is in line with the $I4_1md$ structure reported for more-superstoichiometric samples. In this structure, ideal ordering occurs for $x=0.5$ where the additional D_o atoms above $x=0.25$ occupy specific $D(o3)$ sites.[3,5] As mentioned earlier, this type of ordering was indeed reported for $LaD_{2.30}$.[3]

Although the $I4/mmm$ symmetry of the refined low-temperature $LaD_{2.25}$ structure is in accordance with the TbD_{2+x} results,[16] analysis of the TbD_{2+x} data indicated that it was not necessary to introduce an additional distortion of either the D_t or Tb sublattices to attain good agreement with the ordering model. Moreover, the upper limit for a possible tetragonal distortion was found to be $c_c/a_c < 1.001$. These details were somewhat contrary to our findings for $LaD_{2.25}$ and the similar structural details reported for $CeD_{2.26}$.[5] As a result, we decided to measure for ourselves the NPD patterns for the analogous superstoichiometric compound $TbD_{2.25}$ and refine the structure using the same procedures as for $LaD_{2.25}$. The de-

tails will be reported elsewhere,[25] but the preliminary results for 70 K data confirm a slight tetragonal distortion [$0.5c_T/a_T = 1.000\,67(8)$, with $a_T = 5.2196(1)$ and $c_T = 10.4462(5)$] as well as significant distortions of the D_t and Tb sublattices. For Tb(1) at 4*e* (0,0,*z*) and D(*t*) at 16*n* (*x*,*x*,*z*), model refinement indicated $z = 0.2465(2)$ for Tb(1), and $x = 0.2581(2)$ and $z = 0.1266(2)$ for D(*t*). This is in excellent agreement with the $LaD_{2.25}$ 80 K values, $z = 0.2463(2)$ for La(1), with $x = 0.2591(2)$ and $z = 0.1269(2)$ for D(*t*). Thus the present data indicate that there is indeed total agreement among the structural details of the La, Ce, and Tb deuterides with a D/metal stoichiometric ratio near 2.25. The tetragonal distortion observed for all of these compounds appears to accommodate better the long-range-ordered arrangement of D_o atoms.

The $I4/mmm$ structure is consistent with deuterium NMR data[26] for LaD_{2+x}, which showed that two crystalline electric-field environments were predominant for D at $x = 0.28$, and were assigned to nearly cubic *o* sites and axially symmetric *t* and *o* sites. Each D_o atom possesses a nearly cubic local environment since ideally all the *t* sites are occupied. Conversely, each D_t atom possesses an axially symmetric local environment since the occupation of only D(*o*1) sites in the *o* sublattice provides each D_t atom with one nearest-neighbor D_o atom. If one considers the possibility that even a minute fraction of *t* sites is unoccupied, this means that those D_o atoms neighboring the *t*-site vacancies will also possess axially symmetric local environments. There was evidence from the NMR data for $x = 0.28$ that a small fraction of D atoms possessed a third environment involving strongly asymmetric *t* sites resulting from a pair of occupied neighboring *o* sites. A significant portion of D possessed this latter environment at $x = 0.48$. With respect to the $I4/mmm$ structure, this third environment coincides with the D_t atoms that gain a second D_o neighbor upon adding more deuterium to the $LaD_{2.25}$ *o* sublattice. For the present $LaD_{2.25}$ data, the refinements suggest that for *x* slightly greater than 0.25, the second D_o neighbors occupy D(*o*2) sites. As one approaches the $I4_1md$ structure for $x = 0.50$, the second D_o neighbors occupy select D(*o*3) sites.

There were indications from previous differential scanning calorimetry (DSC) measurements[13] that the transition from cubic to tetragonal symmetry for LaH_{2+x} ($0.1 < x < 0.4$) may occur via a cubic/tetragonal two-phase region. For $LaH_{2.25}$, the tentative DSC-generated phase diagram suggested that the two-phase region existed between ~330 and 295 K. A companion phase diagram derived from x-ray lattice-constant measurements[12,13] failed to identify a two-phase region for $0.2 < x < 0.4$. For $x = 0.23$, the cubic/tetragonal transition occurred near 300 K and the temperature dependence of the tetragonality was reminiscent of a second-order transition; for $x = 0.28$, the transition occurred above 350 K. Our neutron-diffraction data for $LaD_{2.25}$ locate the transition temperature at 345±5 K in line with the x-ray results, and are consistent with the absence of a two-phase region. The fits of the spectra measured near the transition region at 340 K (tetragonal) and 350 K (cubic) could not be improved by any addition of the second phase, suggesting that all spectra represented single phases. Hence, according to our data, this restricts the possible existence of a two-phase region to within a narrow temperature range of 340–350 K.

Figure 4(a) displays the temperature dependence of the lattice parameters. The room-temperature lattice parameters are consistent with the extrapolation of the cubic lattice parameters reported[7] for LaD_{2+x} for $0.27 < x < 1.00$. For the high-temperature cubic and the lowest-temperature tetragonal regions, the increase in the *a* (a_T) and *c* (c_T) lattice constants with temperature is indicative of normal thermal expansion. In contrast, although *a* (a_T) increases monotonically with temperature over the entire range investigated, c_T is maximized at ~230 K followed by a monotonic decrease as the temperature is increased to 345 K. This behavior in the c_T constant is the result of a second process, i.e., the temperature-induced variation in the extent of long-range ordering within the D_o sublattice competing with the effects of normal thermal expansion. In particular, below ~230 K, the long-range order is fully developed; increasing the temperature above 230 K leads to an increase in the disorder within the D_o sublattice concomitant with a relaxation of the order-induced tetragonal distortion (i.e., a contraction of the c_T lattice constant).

The temperature dependence of the c_T/a_T ratio is illustrated in Fig. 4(b), and is in line with the behavior observed by previous x-ray measurements[12] of LaH_{2+x}. The maximum c_T/a_T ratio of 2.0126 was observed at low temperature. This translates into a maximum tetragonality $(0.5c_T - a_T)/a_T$ of 0.63%. The gradual increase in tetragonality with decreasing temperature is concomitant with the gradual development of full long-range order over roughly a 115 K range.

The temperature-dependent changes in atomic positions and D site occupations due to the development of long-range order are plotted in Figs. 4(c) and (d), respectively. Figures 5(a) and 5(b) display the temperature-dependent behavior of the D_o-La and D_t-La bond lengths and the La-D_t-La bond angles. Again, changes in atomic parameters follow a decrease in D_o structural ordering upon increasing the temperature above ~230 K. In particular, both D(*o*2) and D(*o*3) sites become increasingly filled at the expense of the D_o atoms in the D(*o*1) sites. Among other things, this leads to a contraction of the cube of D_t atoms around the D(*o*1) sites and an increase in the D(*o*1)-La(1) bond length. As the high-temperature cubic phase is approached, the different *o* sites become geometrically identical, concomitant with the development of complete disorder in the D_o sublattice.

It is interesting to note that the refined structure of $LaD_{2.25}$ yields a slightly distorted D(*o*1) site at low temperature that has a shorter D_o-La in the *c* direction [D(*o*1)La(1) = 2.780 Å] than in the *ab* plane [D(*o*1)-La(2) = 2.809 Å]. This is similar to the D(*o*1)-site distortion observed for $TbD_{2.25}$. From geometric considerations, one would expect a relative stiffening of the *c*-directed D_o-La force constant compared to that in the *ab*

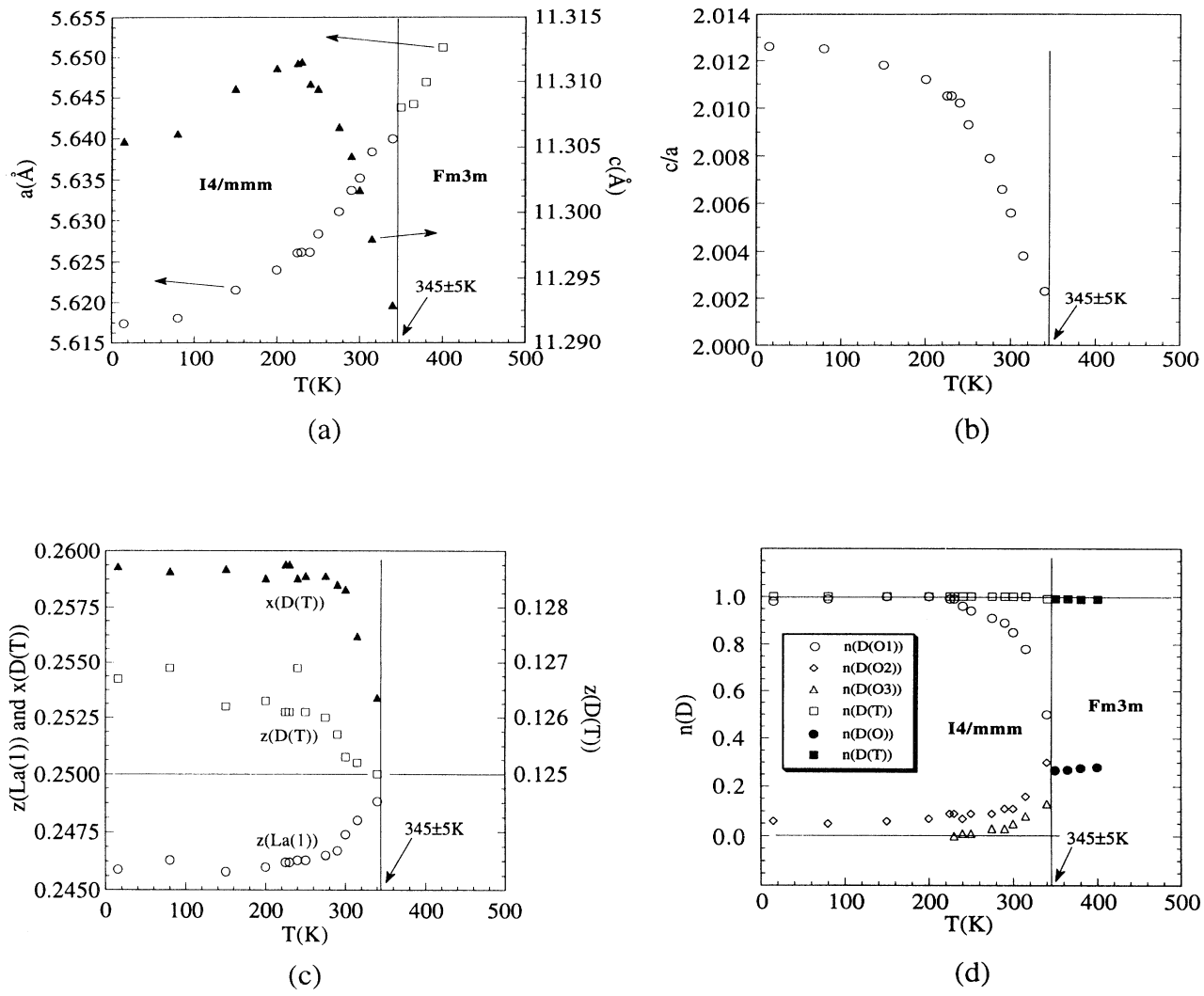

FIG. 4. The temperature dependence of (a) the a and c lattice constants, (b) the c/a ratio, (c) the coordinate shifts for La and D_t, and (d) the D site occupancies. Data are taken from Tables II and III.

plane where the D_o-La distance is larger, leading to a splitting of the D_o vibrational energies. A neutron vibrational spectrum[24] of $LaH_{2.1}$ has indeed shown evidence of a splitting of the H_o optic-vibrational density of states (DOS) at low temperature, although the authors have attributed it to a breaking of cubic symmetry (and therefore vibrational degeneracies) due to an off-center occupation of the o sites. Neutron vibrational spectroscopic results[18] for the ordered H_o sublattice in $TbH_{2.25}$ have also indicated a bimodal DOS. In agreement with intensity and symmetry arguments, the softer mode was assigned to the H_o vibrations along the c direction and the harder mode was assigned to doubly degenerate H_o vibrations in the ab plane. This is contrary to the H_o vibrational mode assignments one would expect from a consideration of the $D(o1)$-site distortion, assuming that the mode energies are dominated by H_o-metal interactions. In addition, recent spectroscopic measurements[27] for $Tb(H_{0.1}D_{0.9})_{2.25}$ indicated that the removal of potential H_o-H_o dynamic coupling interactions by the dilution of H_o atoms with D_o atoms leads to a single H_o vibrational feature devoid of a bimodal line shape. Hence it appears that, at least for TbH_{2+x}, symmetry-dependent, longer-range H_o-H_o dynamic coupling interactions, as opposed to H_o-metal interactions, dominate the H_o vibrational behavior.

It would be informative to compare the H_o DOS for $LaH_{2.25}$ with that for $TbH_{2.25}$. Recently, we reported preliminary neutron vibrational spectroscopic results[27] for $LaD_{2.25}$. The D_o DOS spectrum for $LaD_{2.25}$ exhibited the same bimodal line shape found for $TbH_{2.25}$. Moreover, our latest results[28] indicate that the concentration and temperature dependences of the H_o DOS spectra for LaH_{2+x} are both in agreement with the spectroscopic

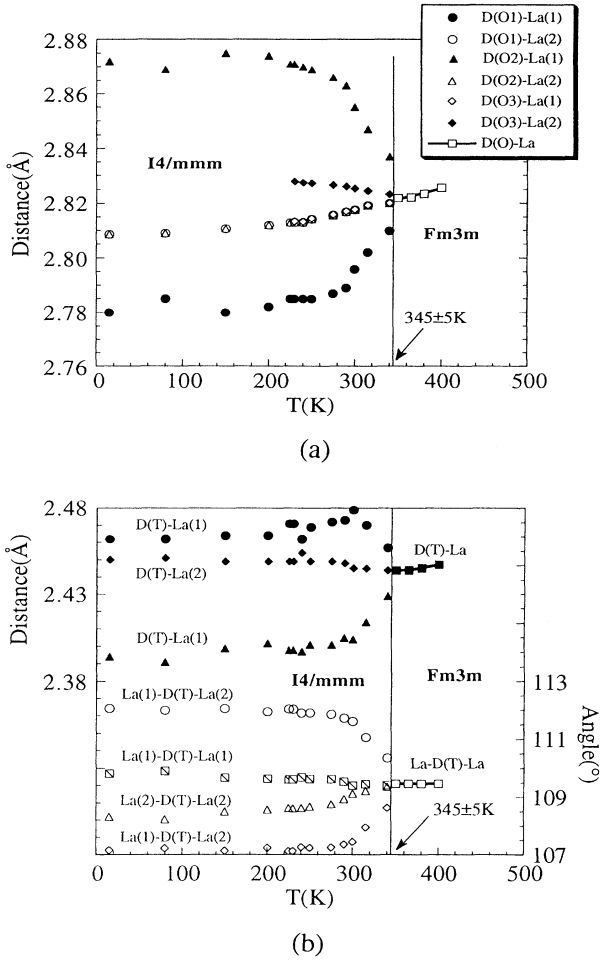

FIG. 5. The temperature dependence of (a) D_o-La interatomic distances and (b) D_t-La interatomic distances and La-D_t-La angles. Data are taken from Table IV.

behavior observed for TbH_{2+x}. Thus, based on the diffraction and spectroscopic results to date, it appears that the long-range ordering tendencies as well as the vibrational dynamics of the H_o atoms are similar in TbH_{2+x} and LaH_{2+x} near $x=0.25$. In order to expand the scope of our measurements, we are currently pursuing more detailed concentration- and temperature-dependent investigations of the H_o (and D_o) ordering tendencies and vibrational dynamics in $La(H/D)_{2+x}$ and other rare-earth hydride systems.

SUMMARY

Temperature-dependent NPD measurements of $LaD_{2.25}$ have been performed. Above ~345 K, the $LaD_{2.25}$ structure is cubic ($Fm3m$), consisting of an fcc La lattice with essentially full deuterium occupation of the t sites and the excess deuterium randomly occupying the o sites. As the temperature is decreased below ~345 K, a transformation from cubic to tetragonal symmetry takes place concomitant with the appearance of D_o long-range order ($I4/mmm$). Fully developed long-range order is established near 230 K and ideally corresponds to the occupation of only those o sites within every fourth (042) plane, in line with structures reported for $CeD_{2.26}$ (Ref. 5) and TbD_{2+x}.[16] This ordering is accompanied by an outward expansion of the cubic ensemble of eight D_t atoms surrounding each D_o atom. Moreover, the c-directed La-D_o bond distances are decreased by a displacement of the La atoms toward the D_o atoms. These results suggest that this structure is more or less common to all the related superstoichiometric rare-earth dideuterides (and didydrides) with D(H)/metal ratios near 2.25 and is believed to be driven by a repulsive interaction between D_o atoms.

It is evident from this and previous studies that the quality of rare-earth-hydride samples, and hence, the reliability of the conclusions drawn from their investigation is highly dependent on the sample purity and synthesis methods. From our own experience as well as others,[29] metal impurities even at the level of 0.1% can cause significant inaccuracies in the targeted stoichiometry. Moreover, care must be taken during the synthesis procedure to further ensure sample purity and homogeneity, even when using high purity materials. Future comparisons of experimental data should include a comparison of the stoichiometry-sensitive lattice constants as an internal check of the quoted metal-hydride stoichiometries.

ACKNOWLEDGMENT

The authors would like to thank Dr. A. Santoro for many helpful discussions.

[1]D. S. Schreiber and R. M. Cotts, Phys. Rev. **131**, 1118 (1963).
[2]A. K. Cheetham and B. E. F. Fender, J. Phys. C **5**, L35 (1972).
[3]C. G. Titcomb, A. K. Cheetham, and B. E. F. Fender, J. Phys. C 7, 2409 (1974).
[4]J.-J. Didisheim, K. Yvon, P. Fischer, W. Hälg, and L. Schlapbach, Phys. Lett. **78A**, 111 (1980).
[5]V. K. Fedotov, V. G. Fedotov, M. E. Kost, and E. G. Ponyatovskii, Sov. Phys. Solid State **24**, 1252 (1982) [Fiz. Tverd. Tela (Leningrad) **24**, 2201 (1982)].
[6]T. Ito, B. J. Beaudry, K. A. Gshneidner, Jr., and T. Takeshita, Phys. Rev. B **27**, 2830 (1983).
[7]P. Klavins, R. N. Shelton, R. G. Barnes, and B. J. Beaudry, Phys. Rev. B **29**, 5349 (1984).
[8]I. O. Bashkin, M. E. Kost, and E. G. Ponyatovskii, Phys. Status Solidi A **83**, 461 (1984).
[9]J. Schefer, P. Fischer, W. Hälg, J. Osterwalder, L. Schlapbach, and J. D. Jorgensen, J. Phys. C **17**, 1575 (1984).
[10]J. P. Burger, J. N. Daou, and P. Vajda, Philos. Mag. B **58**, 349

(1988).
[11]K. Kai, K. A. Gschneidner, Jr., B. J. Beaudry, and D. T. Peterson, Phys. Rev. B **40**, 6591 (1989).
[12]E. Boroch, K. Conder, C. Ru-Xiu, and E. Kaldis, J. Less-Common Met. **156**, 259 (1989).
[13]K. Conder, L. Wang, E. Boroch, E. Kaldis, and J. Schefer, Eur. J. Solid State Inorg. Chem. **28**, 487 (1991).
[14]J. N. Daou, J. P. Burger, and P. Vajda, Philos. Mag. B **65**, 127 (1992).
[15]I. G. Ratishvili, P. Vajda, A. Boukraa, and N. Z. Namoradze, Phys. Rev. B **49**, 15 461 (1994).
[16]G. André, O. Blaschko, W. Schwarz, J. N. Daou, and P. Vajda, Phys. Rev. B **46**, 8644 (1992).
[17]J. W. Ward, B. Cort, J. A. Goldstone, A. C. Lawson, L. E. Cox, and R. G. Haire, in *Transuranium Elements: A Half Century,* edited by L. R. Morss and J. Fuger (American Chemical Society, Washington, DC, 1992), p. 404.
[18]T. J. Udovic, J. J. Rush, and I. S. Anderson, Phys. Rev. B **50**, 7144 (1994).
[19]S. N. Sun, Y. Wang, and M. Y. Chou, Phys. Rev. B **49**, 6481 (1994).
[20]Y. Wang and M. Y. Chou, Phys. Rev. B **49**, 10 731 (1994).
[21]P. Vajda, J. N. Daou, and J. P. Burger, Phys. Rev. B **36**, 8669 (1987).
[22]H. M. Rietveld, J. Appl. Crystallogr. **2**, 65 (1969).
[23]A. C. Larson and R. B. Von Dreele, *General Structure Analysis System* (University of California, Berkley, 1985).
[24]J. A. Goldstone, J. Eckert, P. M. Richards, and E. L. Venturini, Physica **136B**, 183 (1986).
[25]Q. Huang, T. J. Udovic, J. J. Rush, J. Schefer, and I. S. Anderson, J. Alloys Compounds (to be published).
[26]D. G. De Groot, R. G. Barnes, B. J. Beaudry, and D. R. Torgeson, J. Less-Common Met. **73**, 233 (1980).
[27]T. J. Udovic, J. J. Rush, and I. S. Anderson, J. Alloys Compounds (to be published).
[28]T. J. Udovic, J. J. Rush, and I. S. Anderson (unpublished).
[29]J. N. Daou, P. Vajda, J. P. Burger, and A. Lucasson, Phys. Status Solidi A **98**, 183 (1986).